PROBLEMY MECHATRONIKI
UZBROJENIE, LOTNICTWO, INŻYNIERIA BEZPIECZEŃSTWA

ISSN 2081-5891
E-ISSN 2720-5266

14, 1 (51), 2023, 23-60

PROBLEMS OF MECHATRONICS
ARMAMENT, AVIATION, SAFETY ENGINEERING

Methods to Increase the Protective Effectiveness of Add-on Armour made of Perforated Ultra-High-Strength Nanobainitic Steel Plates

Bogdan GARBARZ[1], Jarosław MARCISZ[1*], Wojciech BURIAN[2], Aleksander KOWALSKI[2], Jacek BOROWSKI[3], Szymon SZKUDELSKI[3], Marek WALICKI[4], Kamil ZAJĄC[4]

[1]Łukasiewicz Research Network - Upper Silesian Institute of Technology
12-14 Karola Miarki Str., 44-100 Gliwice, Poland
[2]Łukasiewicz Research Network - Institute of Non-Ferrous Metals
5 Sowińskiego Str., 44-100 Gliwice, Poland
[3]Łukasiewicz Research Network - Poznań Institute of Technology
6 Ewarysta Erdkowskiego Str., 61-755 Poznań, Poland
[4]CFT Precyzja sp. z o.o. (Ltd)
6 Polna Str., 05-152 Czosnów, Poland
Corresponding author's e-mail address and ORCID:
jaroslaw.marcisz@git.lukasiewicz.gov.pl; https://orcid.org/0000-0002-0001-2197

Received: August 3, 2022 / Revised: August 26, 2022 / Accepted: September 1, 2023 / Published: March 31, 2023

DOI 10.5604/01.3001.0016.2958

Abstract. The mechanical properties of industrially produced perforated steel plates are obtained by hardening and low-temperature tempering to produce a martensitic microstructure. Another morphological type of steel microstructure that allows for ultra-high strength and, at the same time, a level of ductility that qualifies it for use in armour is nanobainite. Research into nanobainitic steels has led to the development of plates manufacturing technology at a level that can be implemented in industrial production, and has confirmed the high potential of this material for use as additional armour in the form of perforated plates. This paper reports the results of research aimed at developing a technology for the production of perforated armour plates made of nanobainitic steel, with properties competitive with currently available perforated steel plates on the world market with the highest protective effectiveness under conditions of multi-hit firing tests with small and medium calibre ammunition. The tests were performed on 300 × 260 mm plates, with the nominal thicknesses of 8 mm, 6 mm and 4 mm, produced from industrially melted nanobainitic steel NANOS-BA®. The protective effectiveness of nanobainitic perforated plates in a system with a solid armour steel backing plate of 500 HBW hardness was tested by multi-hit firing, according to the procedures set out in the STANAG 4569 and AEP-55 vol. 1 specifications (adapted to the format of tested plates), against selected projectile types assigned to protection levels 2 and 3. Based on the analysis of the results of the firing tests and the macroscopic and microscopic examinations of the perforated plates before and after firing, the optimum perforation method was selected and the most favourable geometrical and dimensional arrangements of the perforations were determined for different plate thicknesses.
Keywords: add-on armour, perforated plates, ultra-high-strength nanobainitic steel

1. INTRODUCTION

Research and technological work to develop and improve the design of additional armour in the form of perforated plates and multilayer panels incorporating perforated plates has been carried out for more than three decades (the first patents were applied for in 1986, 1989 [1, 2]), and the first scientific publications reporting the results of studies on the ballistic resistance of perforated plates intended for additional armour were published in 2009 / 2010 [3, 4]. Research and development work on perforated armour plate has led to a number of design solutions whose effectiveness has been proven under operational conditions. Perforated armour plates have been classified as standard construction elements (example – MIL-PRF-32269 (MR) [5]), but it is still a product in development.

The main advantages of additional armour in the form of a perforated plate – or a system incorporating perforated plates – over solid plate armour are reduced areal density, increased resistance to crack propagation in the plate and the effects of hole edges interacting with the projectile [6], causing destabilisation of the projectile trajectory and deformation or fragmentation of the projectile core.

Due to their ability to prevent the spread of cracks, perforated panels are particularly suitable for covers used in multi-hit conditions. The perforation pattern designs used different hole shapes (circular, triangular, square, hexagonal and oval-slotted) and different patterns of their arrangement. The modelling, demonstration and final design solutions developed to date for additional armour made of perforated plates, use single plates (examples: [1, 7, 8]) or composite perforated panel systems (examples: [2, 9, 10]). Currently, Perforated Mars®650 [11] and Perforated Miilux® Protection 500 [12] perforated plates are offered by manufacturers of steel products and armouring components in the highest strength class of metal materials. The mechanical properties of these materials are obtained by quenching (and possibly low-temperature tempering) to produce a martensitic microstructure. Another morphological type of steel microstructure that allows ultra-high strength and, at the same time, ductility to qualify for use in armour is nanobainite. The class of nanobainitic steels is a relatively new structural material, currently at the stage of being introduced to industrial-scale manufacturing. The technology has been developed to produce armoured perforated plates from nanobainitic steels (PAVISE™SBS 600P), but – according to the available information – perforated nanobainitic plates are currently not offered as commercial products [13].

The aim of the research to date on the development of the design of additional armouring using perforated plates has been to develop the shapes and dimensions of holes and the patterns of their arrangement, adapted to protection against specific types of projectile, and to select and optimise the properties of the material from which the plates are made. Numerical simulations, physical experiments for isolated types of projectile-armour interactions and verification firing tests are used as test methods. Physical fundamental research and numerical simulations have led to the elucidation of the mechanism of many phenomena occurring during the interaction of the projectile with the perforated plate elements. Due to the complex influence of many factors on the effects of a projectile interacting with a perforated plate, there is still a need for experimental studies performed on model plates in order to search for solutions tailored to particular protective applications. Additional variables to be taken into account in the numerical models and in the interpretation of the physical test results are the inhomogeneity of the properties of the steel plates at the cross-section due to chemical segregation and structural banding – especially in the near-surface layer – and the scatter of the actual dimensions, which for holes up to about 10 mm in diameter, depending on the method and fabrication class, ranges from about ±0.05 mm to about ±0.25 mm [14, 15].

Based on the published results of the research work and technical reports on the influence of geometrical parameters and mechanical properties of perforated metal plates on the mechanisms of interaction with AP small and medium calibre projectiles [3, 4, 6, 9, 10, 16-27], the conclusions given below can be formulated as a basis for identifying areas requiring further research.

The role of the projectile jacket in the mechanism of interaction with armour

The results of the study of the contribution of the jacket and core of the projectile to the mechanism of interaction with armour indicate that the magnitude of the effect associated with the impact of the jacket depends on the type and properties of the armour. In the case of armour with an outer layer of ceramic material, the role of the jacket has been identified as important – a 7.62 mm FFV projectile core without a jacket causes more destruction of the ceramic than a complete projectile [17]. In contrast, the work [3] has found a relatively small contribution from the jacket of a 7.62 mm APM2 bullet fired into aluminium alloy plates of various thicknesses in the range of 20-60 mm. In the case of steel armour plates at which 12.7 mm calibre projectiles are fired, it has been found experimentally and confirmed by numerical simulation results that the jacket increases the penetration capability of the projectile, by absorbing part of the backscattered energy of the projectile-armour interaction and as a result of delaying the scattering of projectile core fragments, in the event of fragmentation [18]. There are no research reports in the available scientific and technical literature on the role of the projectile jacket in the mechanism of interaction with perforated plates. Taking into account the available test results and the fact that the jacket is made of a material with low hardness and its thickness for 7.62 mm calibre bullets is 0.6-0.9±0.05 mm, the diameter of the bullet core is taken as the reference dimension for determining the dimension of holes in perforated armour plates.

Shape, arrangement and size of holes in perforated armour plates

Perforated metal sheets and plates in a wide variety of grades, including material type, sheet or plate thickness and hole shapes, sizes and patterns, are structural products that have been used for a long time and on which perforated armour plates have been modelled. To date, a number of hole shapes and patterns have been used in the research and testing of perforated armour plates. The most commonly used is a line arrangement of circular holes arranged in an equilateral triangle pattern, and less commonly a line arrangement of parallel slotted holes with semicircular ends.

Square, hexagonal and elliptical hole arrangements have also been studied, but no results are available from systematic studies of the effect of hole shape and arrangement on resistance to firing. In the few works where different hole shapes were used, variants were identified that guaranteed the best interaction with the projectile.

For example, the research [10] concerning the circular, oval and hexagonal shaped holes tested, the hexagonal shape was identified as providing the most effective interaction with the projectile, as measured by the angle of deviation of the projectile axis from normal to the plate and the loss of kinetic energy of the projectile.

The work [10] did not describe the morphology of the penetration or the size of the area of the penetrated section of the perforated plate, which is important under conditions of multiple firing. A study [23], of the ballistic resistance of perforated steel plates with circular and square shaped holes found that the effect of the tested hole shape was small. Numerous numerical simulations and physical tests of the effects of the projectile on the perforated plate, as well as verification firing tests, show that the diameter of the circular hole (D), or the cross-sectional dimension of a differently shaped hole, should be close to but smaller than the diameter of the projectile core (d) [4, 20-23, 25]. The value of the ratio (D/d) < 1 depends on the geometrical parameters of the perforated plate and on the design of the projectile.

Methods of making holes in perforated steel plates

Holes in perforated armour plates can be made before final heat treatment or after final heat treatment. In industrial processes, which must ensure the required dimensional accuracy and economic efficiency, the hole-cutting method is selected according to the thickness and mechanical properties of the plate and the shape and pattern of the hole placement. The methods used are machining, laser beam cutting or a jet of aqueous abrasive suspension. The aforementioned hole-cutting methods differently result in changes to the microstructure and properties of the material layers adjacent to the surface and edge of the hole. There is no information in the available literature on the effect of the perforation method on the result of the projectile interaction with the perforated armour plate.

Distance of the add-on armour in the form of a perforated plate from the body armour

The distance of the additional armour from the protected base structure should be as small as possible so as not to limit the manoeuvrability of the vehicles, but large enough to take advantage of the additional dilatation effect as a place to change the trajectory of the projectile's core or its fragments.

In studies on firing small- and medium-calibre ammunition at perforated plates, the distances between the perforated plate and the plate representing the protected structure, measured along the perpendicular to the surface of the plate, were assumed to range from 10 to 100 mm [9, 21, 22]. The longer distances used were due to measurement conditions [25]. In [22], a study of the firing of steel perforated plates with 7.62 × 54 mm B32 AP bullets found that changing the distance between the perforated plate and the baseplate in the range of 10-50 mm, did not significantly affect the effects of the bullet interaction with the armour plate.

On the basis of the analysis of the test results to date, a review article [16] concluded that it was advisable to test contact systems without a gap between the perforated plate and the primary armour.

Required material properties for perforated armour plates

A prerequisite for effective protection against repeated (multi-hit) firing by add-on armour in the form of a perforated steel plate is the ability to inhibit cracks propagating between the holes, thus preventing large areas of the plate from being knocked out, particularly during repeated firing. To meet this condition, the plate material – in addition to a high hardness of more than about 550 HBW – should be characterised by the highest possible ductility [4, 16, 19]. Perforated plates made of steel grades with very high hardness but low ductility [27] are prone to the formation of large-area openings covering the area of several holes (e.g. [25]).

Potential directions to increase protection effectiveness of add-on armour made of perforated steel plates

Base on the summary of research on development of add-on armour made of perforated steel plates given above it could be stated that the research areas not explored enough and offering further possibilities to increase protection effectiveness of perforated armour plates are:

- Improvement in properties of steel used for perforated armour plates causing increase in toughness while ensuring high strength and hardness at approximate range of 580 - 600 HBW.
- Producing in the area adjacent to edges and surfaces of the holes in the perforated plates such type of microstructure which has no tendency for nucleation and propagation of cracks in effect of interaction with projectiles. Properties of material layer adhering to the surface of the holes significantly depend on a method used for making holes in perforated plate.

2. PURPOSE AND SCOPE OF THE STUDY

The aim of the study was to experimentally validate methods to increase the protective effectiveness of add-on armour made of perforated ultra-high-strength nanobainitic steel plates with increased ductility over plates with a martensitic structure. The scope of the study included:

- selection of a nanobainitic steel grade and heat treatment parameters that ensure high hardness in the 550-600 HBW range and, at the same time, sufficiently high ductility to prevent crack propagation, which is an important characteristic of the material for armour used in repeated firing (multi-hit) conditions,
- an analysis of the influence of the hole making method on the microstructure of the material layer adjacent to the hole and on the effects of the perforated plate interacting with the projectile,
- determining the effect of the mutual distance of the holes in the perforated plate on the interaction with the projectile, with a fixed hole diameter close to that of the projectile core.

In Poland, research to date in the design and manufacture of nanobainitic steels with carbon contents up to about 0.6 wt.%, with improved ductility compared to nanobainitic steels with a higher carbon content in the range of 0.8-0.9%, has led to the development of the NANOS-BA® steel class and plate production technology at a level of technological readiness that allows implementation in industrial production [28-31]. Ballistic resistance studies have confirmed the high potential of this material for use as additional armour in the form of perforated plates [32, 33].

The mechanical properties of products made of NANOS-BA® steel grades, following the application of optimised heat treatment for each grade, are as follows: $R_{p0.2}$ > 1300 MPa; R_m > 2000 MPa; A_5 > 12 %; HBW> 580 and KV (10 × 10 mm / at – 40°C) > 12 J. Due to the high carbon content (in the range of 0.55-0.60 wt.%) and a total alloying elements content in the range of 5-8 wt.%, NANOS-BA ® steel grades are difficult to weld.

Test perforated plates were made as part of this work from nanobainitic steel semiproducts manufactured at domestic steel industry plants. The protective effectiveness of the fabricated plates, in a system with a solid armour steel backing plate with a hardness of 500 HBW, was tested by multi-hit firing in accordance with the procedures set out in the STANAG 4569 and AEP-55 vol. 1 specifications (adapted to the format of tested plates), against selected projectile types assigned to protection levels 2 and 3.

3. CHARACTERISTICS OF THE PLATE MATERIAL AND TESTING METHODOLOGY

3.1. Method of manufacturing solid plates

Solid plates were produced from a nanobainitic steel grade with the designation NB-P. The starting material was slabs forged from ingots produced under industrial conditions, with chemical compositions (wt.%): 0.61% C, 1.95% Mn, 1.84% Si, 1.30% Cr, 0.74% Mo, 0.094% V, 0.018% Al, and 0.010% Ti. Slabs of NB-P steel were hot-rolled into plates with a width of approximately 260 mm and nominal thicknesses of 8 mm, 6 mm and 4 mm at Łukasiewicz Research Network - Upper Silesian Institute of Technology (Gliwice, Poland), using equipment included in the line for semi-industrial hot-rolling, thermo-plastic processing and heat treatment (LPS-B) experiments [34]. Immediately after rolling, plate softening was carried out at LPS-B. Units of 300 mm × 260 mm × thickness (4 mm, 6 mm and 8 mm) were cut from the plates for perforation in the softened state or after final heat treatment, with the surface raw after rolling and heat treatment or with the surface cleaned by shot blasting.

3.2. Selection of final heat treatment parameters for NB-P nanobainitic steel plates

Based on the results of the metallographic and mechanical properties tests, the following two options were selected for the heat treatment of NB-P steel plates:

- Two-stage treatment OC1 = austenitisation at 950°C for 30 minutes, cooling to transformation temperature and transformation to nanobainite: 225°C/12h→cooling down 1h→210°C/83h.
- One-step treatment OC2 = austenitisation at 950°C for 30 minutes, cooling to transformation temperature and transformation to nanobainite: 215°C/96h.

The microstructure of heat-treated NB-P steel is a nanocomposite consisting of nanolayer packets of carbide-free bainite and retained austenite in the form of laths or plates of submicron thickness – typically less than 0.1 μm – and polygonal retained austenite grains ranging in size from a few tenths of a micron to a few microns. The resulting values of the parameters measured in the static tensile test and hardness after the OC1 and OC2 treatments are given in Table 1. Based on the results of the tensile test and hardness measurement, it was determined that the more favourable mechanical properties of the nanobainitic steel plates in the NB-P grade were provided by the OC2 variant. Plates heat - treated according to both variants were prepared for firing tests, in order to determine the effect of small changes in mechanical properties on the protective effectiveness of the perforated plates.

Table 1. Tensile test results of flat specimens cut from 8 mm thick plate rolled in LPS-B from NB-P steel and subsequently heat treated according to variants OC1 and OC2; the table shows average values of three specimens for OC1 and four specimens for OC2

Designation of the heat treatment option	Yield stress	Tensile strength	Elongation		Hardness
	$R_{p0.2}$ [MPa]	R_m [MPa]	A [%]	A_{gt} [%]	HV10
OC1	1303	2037	11.l	8.3	590
OC2	1317	2046	12.6	9.8	592

3.3. Metallographic testing methodology

Microstructure investigation and microhardness measurements were carried out on samples cut from perforated plates of NB-P nanobainitic steel with the dimensions 260 × 300 mm and nominal thicknesses: 8 mm, 6 mm and 4 mm, heat treated before or after perforation. The aim of the study was to characterise the metallographic material in layers adjacent to holes made by laser cutting or milling methods. In particular, the research included:

- observations of the macro- and micro-morphology of the cutting surface along the length of the holes and the edges of the holes from the entrance and exit sides of the laser beam or cutting tool,
- identification of micro-cracks and discontinuities on the cut surface and in the adjacent material layer,
- description of the microstructure in the zone adjacent to the cut surface,
- determination of microhardness profiles from the cutting surface, through zones adjacent to the cutting surface, towards the core of the plate, i.e. drawing up the hardness-distance relationship from the cutting surface.

The diagram in Fig. 1 illustrates how test specimens are cut from 40 mm wide strips taken from perforated plates. Metallographic tests and hardness and microhardness measurements (to produce a microhardness profile from the surface of the hole towards the parent material) were carried out on a plane perpendicular to the surface of the plate, on cross-sections of the bridges between the holes, at the locations indicated by the arrows in Fig. 1.

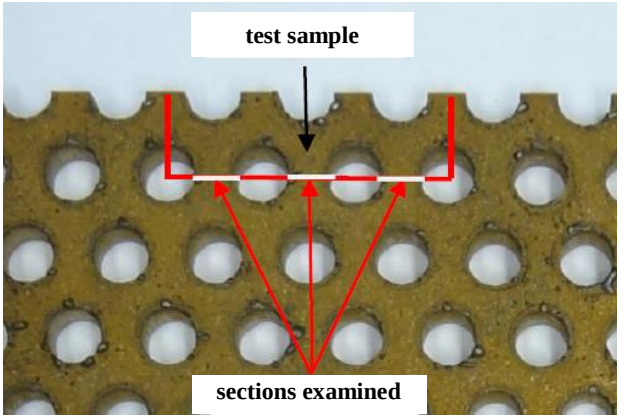

Fig. 1. Method of cutting specimens for metallographic examination from perforated plates

The microstructure of the specimens was observed and imaged on the samples etched in a solution of HNO_3 in ethanol (i.e. in the nital reagent), using light microscopes (MS): optical-digital OLYMPUS DSX500 and NEOPHOT21, and with an Inspect F – FEI scanning electron microscope (SEM). Microhardness and hardness measurements were carried out by means of the Vickers method with load – 200 G (HV0.2) and 10 kG (HV10) using Future-Tech FM-700 micro-hardness tester and a Swiss Max 300 hardness tester respectively, according to certified procedures.

On the basis of the correlations developed between the values of hardness measurements made on samples of nanobainitic steels of the NANOS-BA® class by the Vickers (HV10) and Brinell (HBW) methods, it was found that measurements made by these methods give very similar, almost identical results.

3.4. Methodology of firing tests

Multi-hit firing tests were performed by the CFT Precyzja - Ballistics Laboratory (Czosnów, Poland) in accordance with the requirements of STANAG 4569:ed3:2014, adapted to the size of the samples being tested.

Due to the semi-industrial method of manufacturing the perforated plates, their dimensions are limited to a format of 260 × 260 mm, which limits the number of shots in the multi-hit test. Each of the tested plate systems was fired with four projectiles at points forming two pairs in accordance with Fig. B1 in STANAG 4569/AEP-55 vol. 1, with the distance of the firing points in the pair 25 mm (tolerance -0/+20 mm) and with the distance between the centre point of the first pair and point no. 3 of the second pair equal to 100 mm (tolerance -0/+20 mm). A diagram of the firing test stand is provided in Fig. 2.

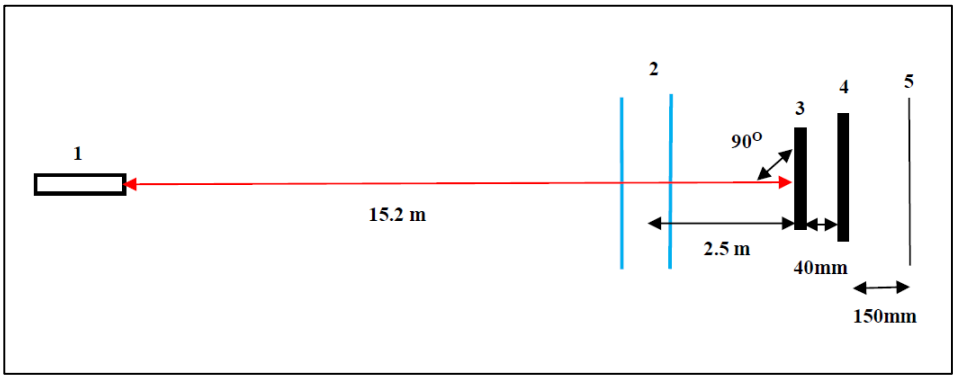

Fig. 2. Schematic of the firing test stand: 1- barrel, 2 – bullet velocity measurement gate, 3 – test perforated plate 260 mm x 260 mm x thickness, 4 – solid base armour plate (500HBW grade) 300 mm x 300 mm x thickness, 5 – aluminium plate 0.5 mm thick ("witness" plate)

Firing was performed according to the direction perpendicular to the surface of the tested plates, at an ambient temperature with a value in the range 18.9-20.6°C. The test plates were positioned so that the firing surface was the entrance surface of the laser beam or cutter when drilling the holes. A distance of 40 mm was established between the perforated plate under test and the solid base plate in all cases, guided by the available results of tests to date of similar armour plate systems and the dimensions of the cores of the projectiles used in tests. For the perforated plate layouts of the tested thicknesses, the following firing parameters were used:

- Perforated plate with a thickness of 4 mm – 40 mm spacing – 500 HBW parallel solid plate with a thickness of 4 mm.
  Level 2 protection against 7.62 × 39 mm API BZ ammunition with a velocity of 695±20 m/s.

- Perforated plate with a thickness of 6 mm – 40 mm spacing – 500 HBW parallel solid plate with a thickness of 6 mm.
  Level 2 protection against 7.62 x 39 mm API BZ ammunition with a velocity of 695±20 m/s.
- Perforated plate with a thickness of 8 mm – 40 mm spacing – 500 HBW parallel solid plate with a thickness of 6 mm.
  Protection level 3 for 7.62 x 54R mm B32 API ammunition with a velocity of 854±20 m/s.

The main criterion for evaluating the result of a multi-hit firing test is the complete penetration or lack of complete penetration of the underlying backing plate. For the test to qualify as positive, none of the four shots must penetrate the base plate. Additional assessment indicators are the size and morphology of the deformation, penetration or tearing of the perforated plate fragments by the projectile, and the type and size of the marks or hole in the underlying solid plate.

4. RESULTS OF INVESTIGATION

4.1. Design of perforation geometry and dimensions and manufacture of perforated plates

Based on the results of a numerical simulation determining the conditions for achieving a uniform probability distribution of induced bending stresses in the projectile core causing core fragmentation [32, 33], a perforation was selected with a circular hole distribution geometry in a passing system on an equilateral triangle pattern, described by these basic parameters: D – diameter of the hole and T – pitch of the perforation pattern, i.e. the distance between the centres of the nearest holes. Figure 3 shows a geometrical diagram of a perforated plate with the perforation parameters indicated, which, in addition to the hole diameter and pattern pitch, are: B – width of the bridge, i.e. the smallest distance between the perimeters of adjacent holes, and Φ – diameter of the circle inscribed in the triangular cell of the hole arrangement pattern. Figure 3 also shows the characteristic points of interaction of a projectile with core diameter d, with a plate.

From the geometric formulas, the following relationships between the parameters describing the perforation pattern in Figure 3 are derived:

$$B = T - D \tag{1}$$

$$\Phi = \frac{\sqrt{3}}{3}\,T = 0.58\,T \tag{2}$$

$$P = \frac{\pi D^2}{2\sqrt{3}\,T^2} \text{ or } P[\%] = \frac{90.69\,D^2}{T^2};\ D, T\ in\ [mm] \tag{3}$$

where P – clearance or open area, i.e. the ratio of the total surface area of the holes to the surface area of the perforated plate.

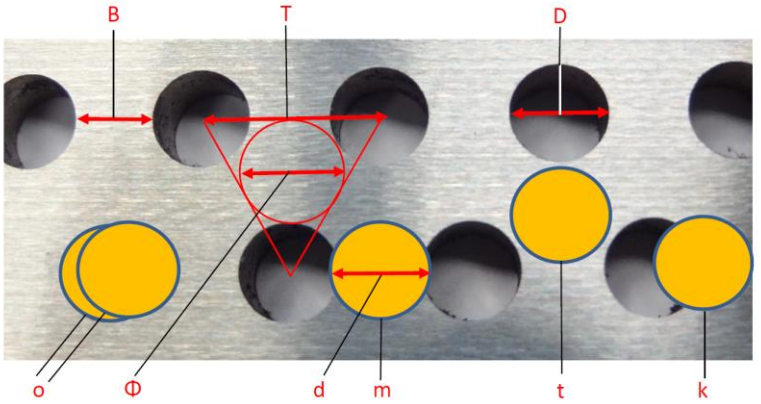

Fig. 3. Determination of the geometrical parameters of a perforated plate, characterising the dimension and arrangement of circular holes in a passing arrangement organised in the pattern of an equilateral triangle: B – bridge, the shortest distance between adjacent holes; T – pitch of the hole pattern, the distance between the centres of adjacent holes; D – diameter of the hole; d – diameter of the projectile core; Φ – diameter of the circle inscribed in the triangular cell of the hole pattern; characteristic locations of the projectile's interaction with the plate: o – axially or non-axially into the hole; m – into the bridge between two holes; t – centrally into the area between three holes (into a triangle), k – into the edge or area adjacent to the edge of the hole

Following the principle derived from the published results of numerical simulations and physical tests performed to date, that the diameter of the hole in the perforated plate should be close to, but smaller than, the diameter of the core, a value of D equal to 6.0 mm was adopted. The dimensions of the projectiles used in the firing tests in this study are as follows:

- 7.62 × 39 mm API BZ ammunition: jacket diameter – 7.88 mm; jacket length – 27.37 mm; core diameter – 6.01 mm; core length – 22.33 mm;
- 7.62 × 54R mm B32 API ammunition: jacket diameter – 7.93 mm; jacket length – 37.96 mm; core diameter – 6.03 mm; core length – 28.32 mm.

In order to investigate the achievable reduction in areal density of the perforated plate, two significantly different pitch values were adopted for the study: T_1 = 10.5 mm (Per 1 designation) and T_2 = 8.5 mm (Per 2 designation) – Fig. 4. For the adopted value of D = 6.0 mm, the geometrical parameters of the designed perforations are as follows:

- Per 1, T_1 = 10.5 mm, B_1 = 4.5 mm, Φ_1 = 6.09 mm, P_1 = 29.6%;
- Per 2, T_2 = 8.5 mm, B_2 = 2.5 mm, Φ_2 = 4.93 mm, P_2 = 45.2%.

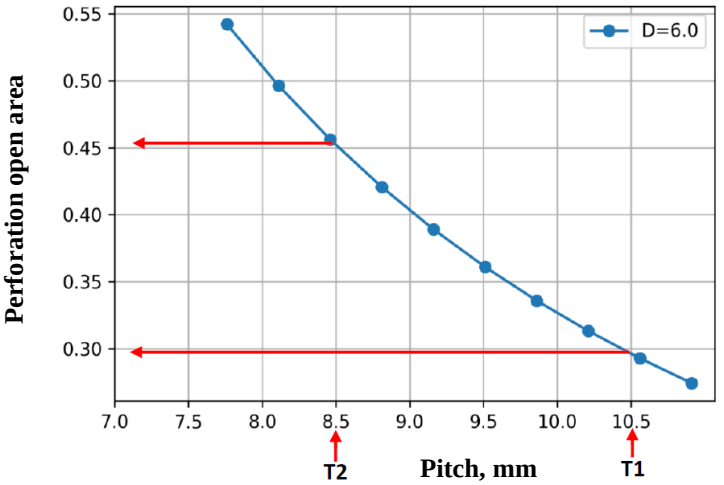

Fig. 4. The value of open area *P* of a perforated plate with holes of 6 mm diameter as a function of the pitch *T* according to formula (3), with the marked values corresponding to the designed patterns, Per 1 and Per 2

Holes were made in 260 × 300 mm NB-P steel solid plates with thicknesses of 4 mm, 6 mm and 8 mm, prepared as described in subsection 3.1, according to the Per 1 and Per 2 pattern designs, by milling (designation *F*) and by laser cutting using oxygen (designation *L*1) or nitrogen (designation *L*2) as the process gas. Holes were cut in plates in the softened state, before the final heat treatment and in plates after the final heat treatment. After the holes were drilled, 40 mm wide strips were cut from the plates to be used as samples for metallographic testing. Table 2 provides a summary and description of the NB-P nanobainitic steel perforated plates prepared for the firing tests.

Table 2. Parameters of the perforated plates prepared for firing tests; plate format 260 × 260 mm.

#	Plate designations	Plate thickness g [mm]	Variant heat treatment	Method performances holes	Perforation pattern D^T [mm]	Open area P [%]	Protection level according to STANAG 4569 and AEP-55 vol. 1 Firing test type
1	6-2f	5.6-5.8	OC1	F after OC1	Per 1: 6.0^10.5	29.6	Level 2 protection against 7.62 x 39 mm API BZ ammunition with a velocity of 695±20 m/s for a perforated plate arrangement and a class 500 HBW solid armour plate with a thickness of 6 mm
2	6-3f	5.6-5.7	OC1	L1 after OC1	Per 1: 6.0^10.5	29.6	
3	6-4f	5.7-5.9	OC1	F after OC1	Per 2: 6.0^8.5	45.2	
4	6-3z-f	5.7-5.8	OC2	L1 before OC2	Per 1: 6.0^10.5	29.6	
5	6-4z-f	5.7-5.9	OC2	F before OC2	Per 2: 6.0^8.5	45.2	
6	6Af	5.2-5.6	OC1	L2 after OC1	Per 2: 6.0^8.5	45.2	
7	6Az-f	5.6-6.0	OC2	L2 before OC2	Per 1: 6.0^10.5	29.6	
8	6-5f	5.9-6.0	OC2	L2 after OC2	Per 1: 6.0^10.5	29.6	
9	6-6f	6.2-6.3	OC2	L2 after OC2	Per 2: 6.0^8.5	45.2	
10	6-7f	6.1-6.3	OC2	F after OC2	Per 1: 6.0^10.5	29.6	
11	4-3f	4.2-4.3	OC1	F after OC1	Per 1: 6.0^10.5	29.6	Level 2 protection against 7.62 x 39 mm API BZ ammunition with a velocity of 695±20 m/s for a perforated plate arrangement and a 4 mm thick solid armour plate of class 500 HBW
12	4-4f	4.2-4.3	OC1	F after OC1	Per 2: 6.0^8.5	45.2	
13	4-3z-f	4.4-4.6	OC2	L1 before OC2	Per 1: 6.0^10.5	29.6	
14	4-4z-f	4.1-4.3	OC2	F before OC2	Per 2: 6.0^8.5	45.2	
15	4-5f	4.4-4.5	OC2	L2 after OC2	Per 1: 6.0^10.5	29.6	
16	4-6f	4.4-4.6	OC2	L2 after OC2	Per 2: 6.0^8.5	45.2	
17	4-7f	4.3-4.4	OC2	F after OC2	Per 1: 6.0^10.5	29.6	
18	8-2f	8.0-8.2	OC1	F after OC1	Per 1: 6.0^10.5	29.6	Protection level 3 for 7.62 x 54R mm B32 API ammunition with a velocity of 840-860 m/s for the perforated plate system and class 500 HBW solid armour plate with a thickness of 6 mm
19	8-3f	7.8-8.0	OC1	L1 after OC1	Per 1: 6.0^10.5	29.6	
20	8-4f	8.0-8.1	OC1	F after OC1	Per 2: 6.0^8.5	45.2	
21	8-2z-f	7.5-7.6	OC2	F before OC2	Per 1: 6.0^10.5	29.6	
22	8-4z-f	7.5-7.7	OC2	F before OC2	Per 2: 6.0^8.5	45.2	
23	8-5f	7.7-7.8	OC2	L2 after OC2	Per 1: 6.0^10.5	29.6	
24	8-6f	7.5-7.7	OC2	L2 after OC2	Per 2: 6.0^8.5	45.2	
25	8-7f	7.7-8.0	OC2	F after OC2	Per 1: 6.0^10.5	29.6	

Indications in the table: g – actual thickness of plates with nominal thicknesses of 6 mm (no. 1-10), 4 mm (no. 11-17) and 8 mm (no. 18-25); D-nominal diameter of the holes, T-nominal distance between the centres of the nearest holes, P-clearance or open area (ratio of the total surface area of the holes to the surface area of the plate), OC1, OC2 – variants of the final heat treatment, F-milling of the holes, L1- cutting of the holes with a laser beam with process gas O_2, L2- laser beam hole cutting with process gas N_2.

4.2. Macro- and microstructure of perforated plates before firing tests

4.2.1. Plates with holes made after final heat treatment by laser beam cutting

The designations of the plates in which the laser beam holes were made after the final heat treatment are as follows (Tab. 2): 6-3f, 6Af, 6-5f, 6-6f, 4-5f, 4-6f, 8-3f, 8-5f and 8-6f.

Macro-morphology of the cutting surface

When holes are cut with a laser using oxygen or nitrogen as the process gas, grooves are created on the cutting surfaces by the cutting beam – an example is shown in Fig. 5a, and material sticking occurs at the bottom of the holes as a result of the molten metal trickling down. SEM images of the hole surfaces show, at high magnifications, the dendritic structure of the solidified metal layer and interdendritic microcracks – Fig. 5b. On cross-sections perpendicular to the surface of the perforated plate, the edges marking the longitudinal profiles of the holes have irregular shapes, and the layers visible after etching, formed as a result of remelting and phase transformations, are characterised by uneven thicknesses along the length of the hole.

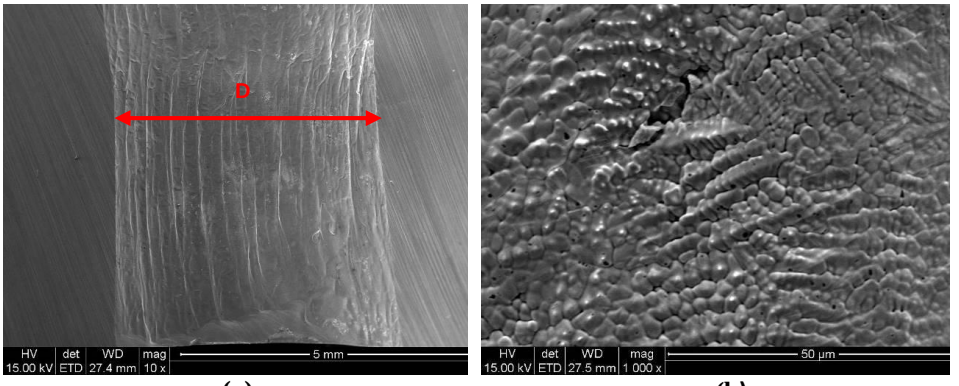

(a) **(b)**

Fig. 5. Examples of SEM images of the surface of a hole cut by a laser beam at low – (a) and high (b) magnification; Plate 8-5f/Per1/L2

Microstructure of the material in the zone adjacent to the cutting surface

The areas of the plate adjacent to the surface of the holes cut by the laser beam consist of the three layers highlighted in the microphotographs in Fig. 6: 1 – remelted layer, 2 – martensitic layer formed by heating to the austenite stability range and rapid cooling, and 3 –parent plate material with nanobainite and retained austenite structure.

The remelted layer is not present over the entire cut surface and is characterised by an uneven thickness along the direction from the top surface to the bottom surface of the plate, with a thickness in the upper and middle sections of the holes in the approximate range of 10-100 μm, while it is thicker, up to 300 μm, in the lower section of the holes. Locally, the remelted layer is not bonded to the substrate. The substructure of the remelted layer consists of ultra-fine plates of martensite – Fig. 6 b. The martensitic layer is present along the entire length of the hole and its thickness is in the approximate range of 100-250 μm. The remelted layer produced by laser beam cutting using nitrogen as the process gas has a lower thickness than the remelted layer produced by laser cutting using oxygen. The thickness of the heat-affected zone with martensitic structure produced by laser cutting using nitrogen as the process gas is comparable to that of the martensitic layer obtained after laser perforation using oxygen. No microcracks were found in the remelted layer or in the martensitic layer on the cross sections.

The 250-350 μm-thick near-surface layer of the plate undergoes partial decarburisation during hot-rolling and heat-treatment processes. This is a typical feature of armour steel plates, as the decarburised thin layers on both sides of the plates are not removed for technological and economic reasons. Due to the resulting surface decarburisation, the edges of the holes are characterised by a lower hardness than that of the layers adjacent to the hole surface below the decarburised layer.

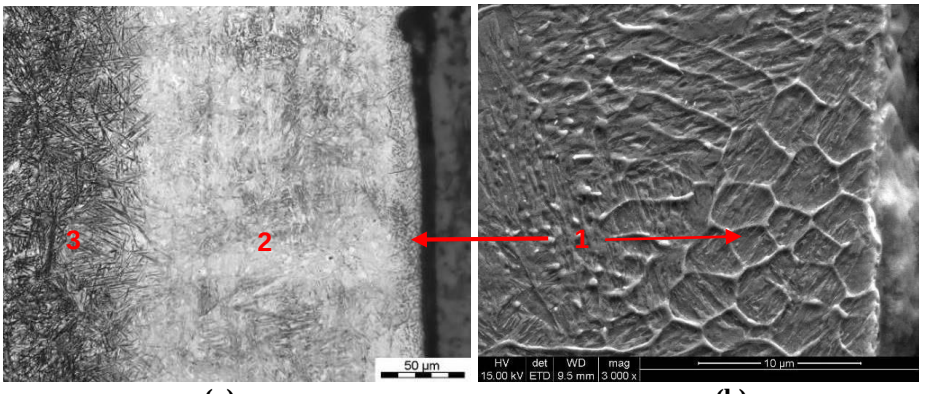

(a) **(b)**

Fig. 6. Microstructure of the layers in the area adjacent to the surface of the hole in the middle of the plate thickness, made by laser method L2 in plate 6-6f; 1 – remelted layer, 2 – martensitic layer, 3 – nanobainite in the parent material; (a) – MS image, (b) – SEM image

Microhardness profiles in the zone adjacent to the laser beam cutting surface

The HV0.2 microhardness profiles determined along a line from the surface of the hole and the edges of the holes, through the microstructural layers produced by laser cutting, to the parent material, are characterised by similar shape and microhardness values at specific distances from the surface – both for profiles determined for the same plate and for profiles determined for plates of different thicknesses. There is a continuous transition between the remelted layer and the martensitic layer with a slight decrease in hardness, while from the martensitic layer through the intermediate zone to the parent material, the hardness decreases more. The microhardness of the remelted layer is in the range at 700-755 HV0.2 (or HV0.1 for the thinnest layers). The microhardness of the martensitic layer, as read from the profiles, is between 700 and 725 HV0.2 for OC1-treated plates and between 750 and 775 HV0.2 for OC2-treated plates. The microhardness of the parent material immediately downstream of the transition zone is 560-570 HV0.2 for OC1 heat-treated plates and 575-605 HV0.2 for OC2 heat-treated plates.

Representative examples of the microhardness profiles and microphotographs of the areas of the plates where measurements were taken are included in Figs. 7 and 8. The initial parts of the microhardness profiles in the hole edge areas are characterised by a lower value than the initial parts of the microhardness profiles in the area adjacent to the hole surfaces, which is due to partial decarburisation of the near-surface layer of the plates. The lowest measured microhardness values in the corner area at a depth of up to 0.2 mm from the surface are 420-430 HV0.2.

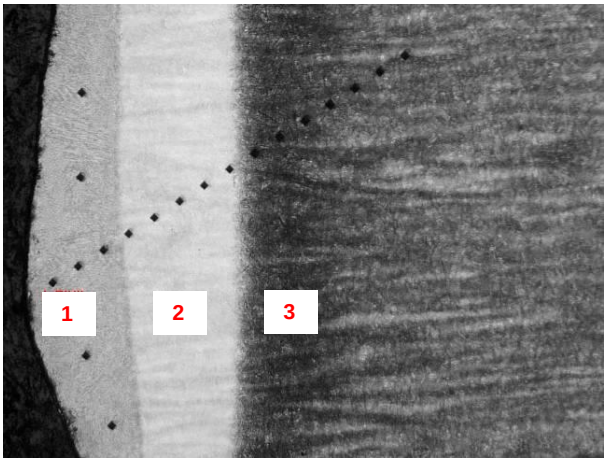

(a)

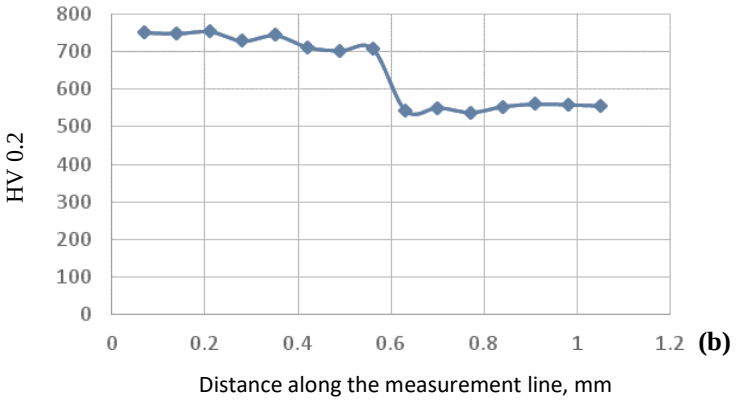

Fig. 7. (a) – MS photograph of an etched section perpendicular to the surface of the 8-3f plate after OC1 heat treatment in the area adjacent to the surface of the hole made by the L1 laser cutting method, with visible imprints after HV0.2 microhardness measurements, (b) – microhardness profile determined along the line visible in microphotograph (a)

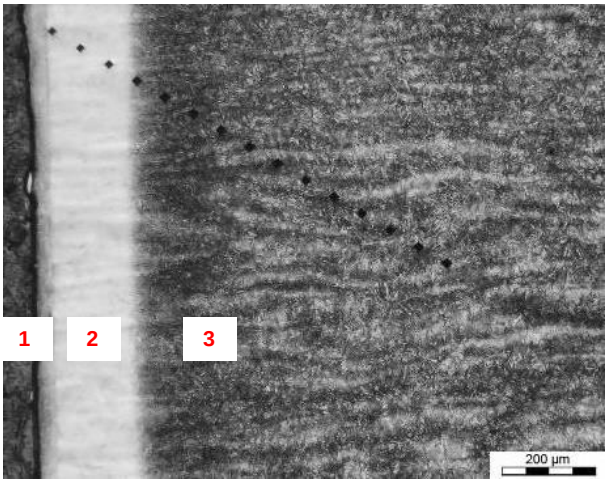

(a)

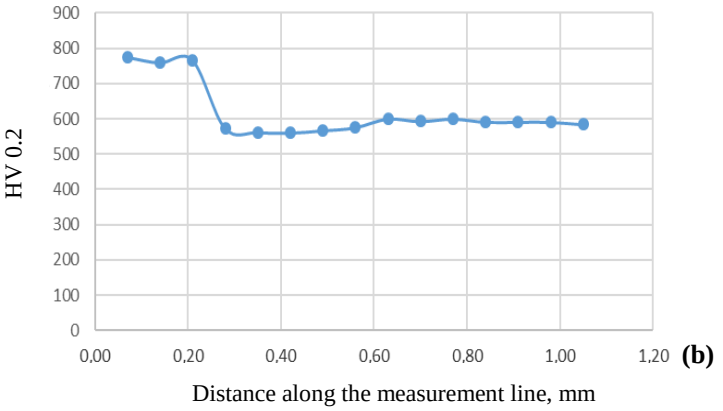

Fig. 8. (a) – MS photograph of the etched section perpendicular to the surface of the 8-5f plate after OC2 heat treatment in the area adjacent to the surface of the hole made by the L2 laser cutting method, with visible imprints after HV0.2 microhardness measurements, (b) – microhardness profile determined along the line visible in microphotograph (a)

4.2.2. Plates with holes made after final heat treatment by milling

Using the milling method, holes were made in the plates after the final heat treatment with the following designations (Tab. 2): 6-2f, 6-4f, 6-7f, 4-3f, 4-4f, 4-7f, 8-2f, 8-4f and 8-7f.

Surfaces of holes made in heat treated plates by machining– in this case by milling – are characterised by low roughness, and the profiles of the intersection of the hole surface with a plane perpendicular to the plate surface are rectilinear, with local irregularities. The production of holes by machining, under conditions that do not cause heating above approximately 150°C, does not induce changes in the microstructure and properties of the starting material in the zones adjacent to the edges and surfaces of the holes. Figure 9 shows example photographs of the microstructure of the plate material in the area adjacent to the hole surface, showing nanobainite with a morphology unchanged from the parent material. Only in layer thicknesses below about 5 μm plastic deformation effects were detected (OP in Fig. 9 b). In the area of the hole edges, due to surface decarburisation, the hardness of the material is lower than at the hole surface at a greater depth than the extent of the partial decarburisation.

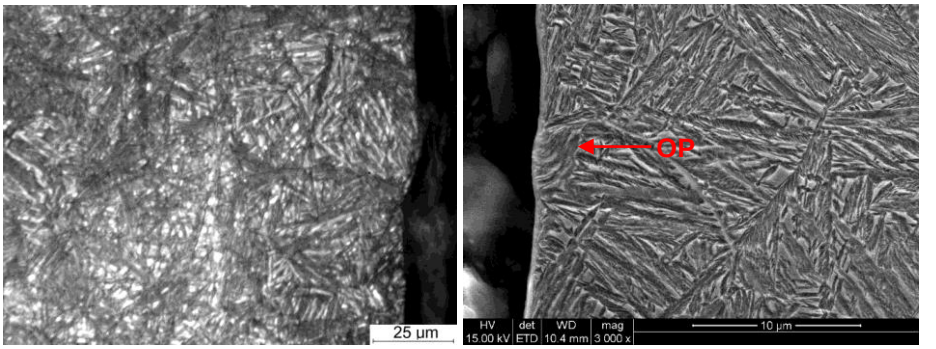

(a) **(b)**

Fig. 9. Microstructure of the layer in the area adjacent to the surface of the milling holes: (a) – Plate 8-4f, MS, (b) – Plate 8-2f, SEM; OP – plastic deformation

4.2.3. Plates heat treated after making holes by laser beam cutting and milling

Plates perforated in the softened state by laser beam cutting and subsequently heat treated have the designations 6-3z-f, 6Az-f and 4-3z-f, while plates perforated in the softened state by milling and subsequently heat treated have the designations 6-4z-f, 4-4z-f, 8-2z-f and 8-4z-f (Tab. 2). The austenitisation of the perforated plates at 950°C for 30 minutes, included in the final heat treatment, resulted in partial decarburisation of the material layer adjacent to the surface of the holes. In the edge area, the effects of decarburisation resulting from the final heat treatment process and primary surface decarburisation resulting from the hot-rolling process are superimposed. Heating to the austenite stability temperature removed the transformation effect caused by the laser beam. During the cooling from the austenitising temperature to the isothermal transformation temperature and as a result of this transformation, various morphological forms of bainite and martensite – rather than nanobainitic structure – were formed in the partially decarburised layer. The type and morphology of the microstructure resulting from the final heat treatment in the layers adjacent to the surface of the holes is similar in laser-perforated plates (Fig. 10) and in plates with milled holes (Fig. 11). The thickness of the partially decarburised layer near the surfaces of the holes is in the range 300-450 µm, and on small areas there has been complete decarburisation to a depth of 20-30 µm resulting in the formation of pre-eutectoid ferrite grains. Along some austenite grain boundaries, shallow internal oxidation has occurred.

The HV0.2 microhardness profiles drawn for the heat-treated plates after the holes were made were determined in the edge area and along a line from the hole surface to the parent material.

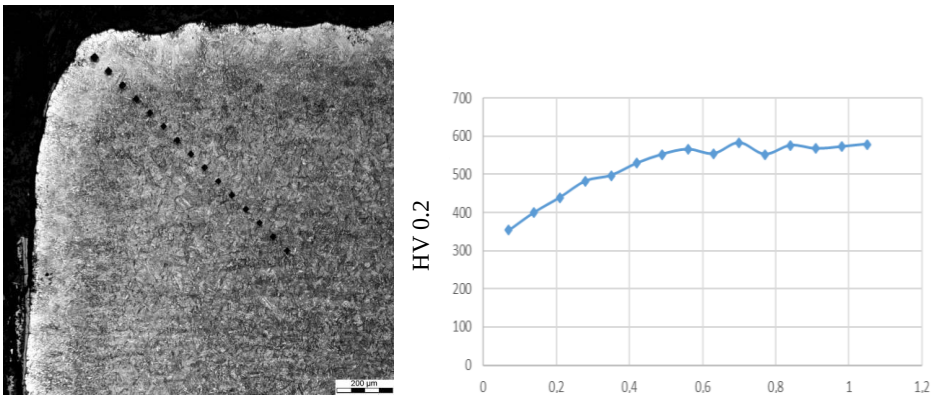

(a) **(b)**

Fig. 10. (a) – MS photograph of an etched section perpendicular to the surface of an 8-3z-f plate perforated by L1 laser beam cutting in a softened state – after perforation the plate was heat treated according to variant OC2; (b) – HV0.2 microhardness profile determined from the impressions visible in photograph (a)

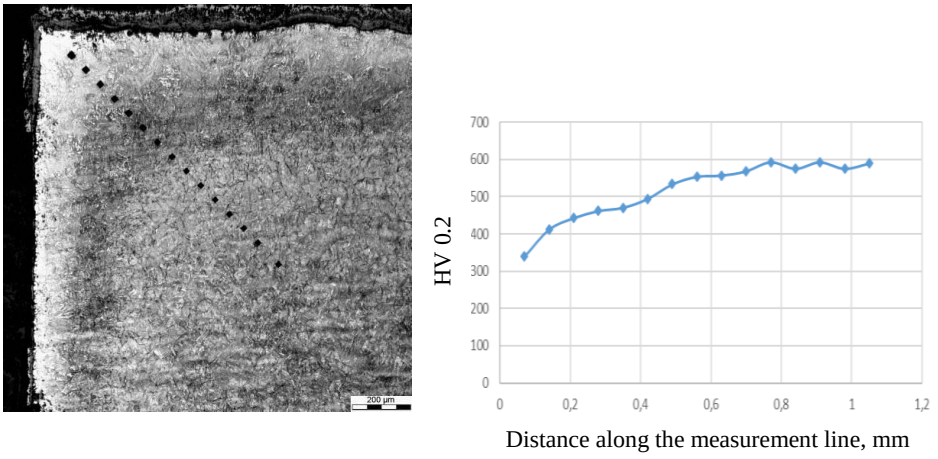

(a) **(b)**

Fig. 11. (a) – MS photograph of an etched section perpendicular to the surface of an 8-4z-f plate perforated by milling in a softened state – after perforation the plate was heat treated according to variant OC2; (b) – HV0.2 microhardness profile determined from the impressions visible in photograph (a)

Heat treatment after perforation, causing decarburisation in the edge area and in the layer adjacent to the surface of the holes, is the reason for the reduction in hardness of these areas in relation to the core of the plate. The lowest measured microhardness in the edge area is in the range 340-410 HV0.2, and the lowest microhardness in the layer adjacent to the hole surface is 370-480 HV0.2.

Microhardness measured along the diagonal on the edge section extends to a depth of approximately 0.8 mm, and along a line perpendicular to the surface of the hole extends to a depth of 0.25 – 0.35 mm. In the edge area, the effects of decarburisation in the final heat treatment process and primary surface decarburisation from the hot-rolling process are superimposed. For these reasons, the initial parts of the microhardness profiles in the edge area are characterised by a lower value than the initial parts of the microhardness profiles in the area adjacent to the hole surfaces.

The heat treatment of the perforated plates caused a deformation, consisting of a deviation from flatness in the corner area relative to the central area of the plate. The maximum deviation from flatness measured at the corner is between 2.5 and 3.5 mm.

4.3. Results of firing tests

4.3.1. Firing tests of structure consisting of 6 mm thick perforated plate and the 6 mm thick armour solid plate 500 HBW with 7.62 × 39 mm API BZ ammunition within the scope of protection level 2 according to STANAG 4569

Table 3 summarises the results of multi-hit firing tests on perforated plates of NB-P nanobainitic steel with a nominal thickness of 6 mm (actual thicknesses are given in Tab. 2), in terms of protection level 2 according to STANAG 4569 for firing 7.62 × 39 mm API BZ ammunition. Ten perforated plates with holes made by milling (F) or laser beam cutting (L1, L2) were tested, using two distances between the centres of the nearest holes: 10.5 mm (T_1) and 8.5 mm (T_2). The areal density (MP) of a solid plate with a thickness of 6 mm is 47.1 kg/m^2, while a perforated plate with parameters [g = 6 mm / D = 6 mm / T = 10.5 mm, ρ = 7.85 g/cm^3] has an MP value of 33.2 kg/m^2, and the plate with parameters [g = 6 mm / D = 6 mm / T = 8.5 mm, ρ = 7.85 g/cm^3], has an MP value of 25.8 kg/m^2.

In the case of the firing of 6 mm thick perforated plate systems with the parameters given in Tab. 3 with a 6 mm thick class 500 HBW solid plate, all multi-hit firing tests with 7.62 × 39 mm API BZ ammunition were qualified as positive. The effects of the interaction of the projectile with the perforated plate and the type and size of the marks on the surface of the baseplate depend significantly on the mechanical properties of the plate resulting from the type of heat treatment applied and the method of making the holes, as well as on the characteristic spot on the perforated plate where the projectile has hit.

Table 3. Summary of the results of multiple-shot (multi-hit, STANAG 4569) tests of perforated plates of nanobainitic steel with a nominal thickness of 6 mm in a base plate arrangement; the ordinal number and designations of the tested plates, heat treatments and hole making methods – as in Table 2; test result: number of shots not penetrating the solid base plate (+) and number of shots penetrating the solid base plate (-)

Shooting test type	**#**	**Plate design.**	**Pattern D∧T [mm]**	**Test result**	**Traces of the impact of successive bullets on the perforated plate, depending on the point of impact marked in Fig. 3: o- hole, m-bridge, t-triangle, k-edge, n-no possibility of identifying the place, op-plastic deformation**
Firing of the system: 6 mm perforated plate and 6 mm armor solid plate 500 HBW with 7.62 x 39 mm ammunition API BZ in protection level 2 according to STANAG 4569	1	6-2f/F after OC1	Per 1: 6.0∧10.5	+ 4(+)	k- edge op, no cracks m- knockout of bridge, op edge of the tear m- knockout of bridge, op edge of the tear k/o- op edges, no cracks
	2	6-3f/L1 after OC1	Per 1: 6.0∧10.5	+ 4(+)	n- brittle breakage of the 5-hole area, cracks n- brittle breakage of the 4-hole area, cracks n- brittle breakage of 2 bridges, cracks n- brittle breakage of the 4-hole area, cracks
	3	6-4f/F after OC1	Per 2: 6.0∧8.5	+ 4(+)	m/t- knockout of bridges in 4-hole area, op of edges t- knockout of bridges in the 3-hole area, op of edges k- edge and bridge op, no cracks t- knockout of bridges in the 3-hole area, op of edges
	4	6-3z-f/L1 before OC2	Per 1: 6.0∧10.5	+ 4(+)	t- knockout of bridges in the 3-hole area, op of edges t- knockout of bridges in the 3-hole area, op of edges k- edge op, no cracks m- knockout of bridge, op edge of the tear
	5	6-4z-f/F before OC2	Per 2: 6.0∧8.5	+ 4(+)	t- knockout of bridges in the 3-hole area, op of edges n- plastic breakout of the area between the 4 holes k/o- op edges, no cracks t- knockout of bridges in the 3-hole area, op of edges
	6	6Af/L2 after OC1	Per 2: 6.0∧8.5	+ 4(+)	n- brittle-plastic knockout fragment comprising 6 holes n- brittle-plastic punching of a fragment involving 5 holes n- brittle-plastic punching of a fragment involving 10 holes n- brittle-plastic punching of a fragment involving 7 holes
	7	6Az-f/L2 before OC2	Per 1: 6.0∧10.5	+ 4(+)	k/m- significant edge and bridge op, no cracks m- knockout of bridge, op edges of tear, no cracks m- knockout of bridge, op edges of tear, no cracks k- significant edge op, no cracks
	8	6-5f/L2 after OC2	Per 1: 6.0∧10.5	+ 4(+)	t- brittle-plastic knockout of bridges in the 3-hole area k/t- brittle-plastic knockout of bridges in area of 3 holes k- op cracks in two bridges t- brittle-plastic knockout of bridges in the 3-hole area
	9	6-6f/L2 after OC2	Per 2: 6.0∧8.5	+ 4(+)	m/t- brittle-plastic knockout of 2 bridges, cracks n- brittle-plastic knockout involving 8 bridges t/m – brittle knockout of bridges in the 4-hole area n- t/m- brittle knockout of fragment of 5 holes
	10	6-7f/F after OC2	Per 1: 6.0∧10.5	+ 4(+)	k- significant edge op, no cracks, small breakage t- plastic knockout of bridges in the 3-hole area m- knockout of bridge, op edges of tears , no cracks k- significant edge op, no cracks

In plates with higher or the same ductility of the material adjacent to the hole compared to the material of the centre of the plate, when the projectile hits the edge of the hole or close to the edge of the hole (position *k* in Fig. 3), local plastic deformation occurs and – in some cases – small tears of material are produced in the impact area (examples: shot 1 in Fig. 12a, b and shot 3 in Fig. 13b). Depressions and craters of varying sizes and depths are formed on the solid base plate and, in cases of deep craters, there is also bulging of the plate. The effect of a projectile striking the area of a bridge or triangle bounded by three holes (positions *m*, *t* in Fig. 3), is to tear or at least to tear a small area involving plastic deformation, such as the effects of shot 2 in Fig. 12a, b and shot 4 in Fig. 13a, b. The impact of the projectile centrally in the hole or close to the centre of the hole (position o in Fig. 3) causes strong plastic deformation of the material adjacent to the hole (as in shot 3 in Fig. 13a) and a concentrated or single crater on the surface of the base plate and its bulge.

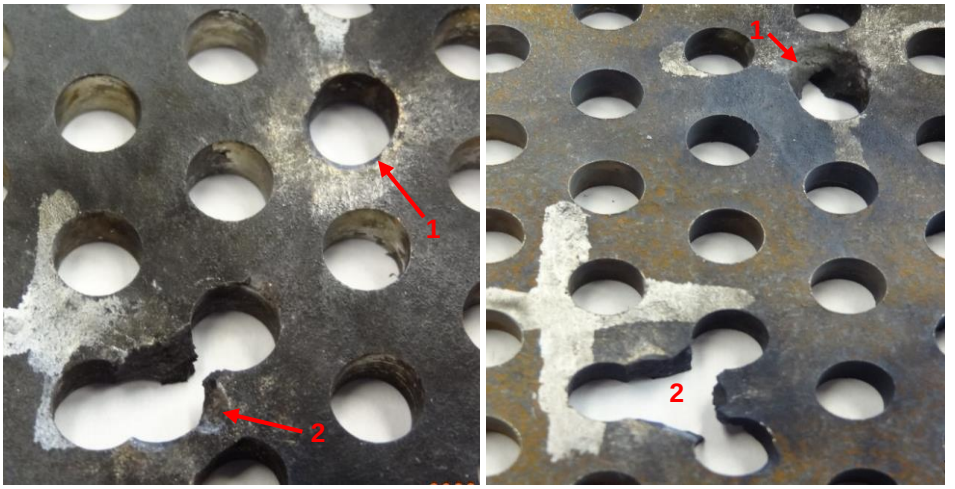

(a) **(b)**

Fig. 12. (a) – plate 6-2f / Per 1-F after OC1: shots 1 and 2 / front surface, (b) – plate 6-7f /Per 1-F after OC2: shots 1 and 2 / front surface

The firing of perforated plates, characterised by reduced ductility and higher hardness of the material adjacent to the holes compared to the ductility and hardness of the central area of the plates, results in brittle-plastic bridge break-outs with cracks in the adjacent bridges or brittle material break-outs covering an area of several to ten holes (Fig. 14). Fragmentation of the plate area, which includes several holes, results in scattered dents of varying depths or individual deep craters and bulges on the base plate. The type of marks on the surface of the baseplate is probably related to the size of the broken fragments of perforated plate.

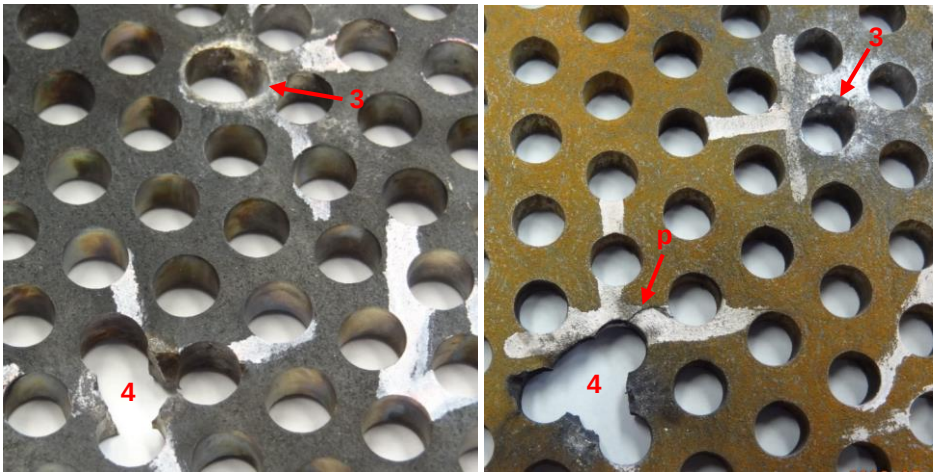

(a) **(b)**

Fig. 13. (a) – Plate 6-4f /Per 2-F after OC1: shots 3 and 4 / front surface,
(b) – Plate 6-5f /Per 1-L2 after OC2: shots 3 and 4 / front surface; p –cracks in bridges

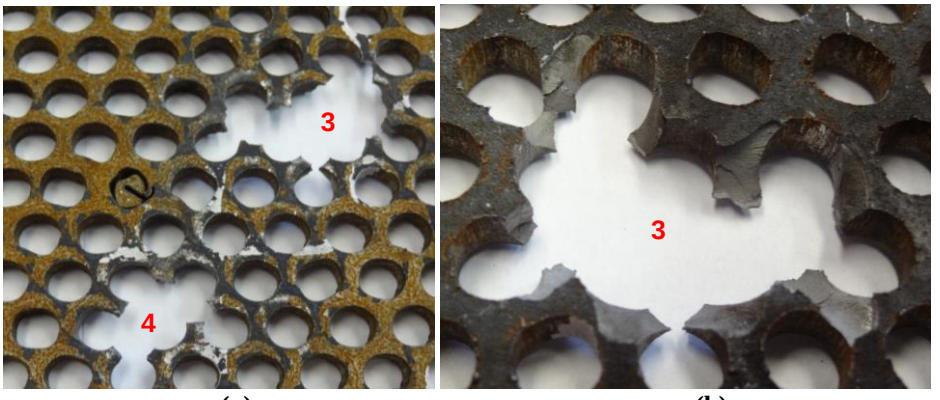

(a) **(b)**

Fig. 14. Plate 6Af /Per 2-L2 after OC1: (a) – Shots 3 and 4 / front surface, |
(b) – Shot 3 / rear surface, enlarged image

4.3.2. Firing tests of structure consisting of 4 mm thick perforated plate and the 4 mm thick armour solid plate 500 HBW with 7.62 × 39 mm API BZ ammunition within the scope of protection level 2 according to STANAG 4569

The results of the multi-hit firing tests of seven perforated plates of NB-P nanobainitic steel with a nominal thickness of 4 mm (actual thicknesses are included in Tab. 2), in terms of protection level 2 according to STANAG 4569 for firing 7.62 × 39 mm API BZ ammunition, are given in Table 4.

Holes in the plates were made by milling (F) or by laser beam (L1, L2), using a distance between the centres of the nearest holes of 10.5 mm (T_1) or 8.5 mm (T_2). The areal density of a 4 mm thick solid plate of NB-P steel is 31.4 kg/m^2, while a perforated plate with parameters [g = 4 mm / D = 6 mm / T = 10.5 mm, ρ = 7.85 g/cm^3] has an MP value of 22.1 kg/m^2, and the plate with parameters [g = 4 mm / D = 6 mm / T = 8.5 mm, ρ = 7.85 g/cm^3], has an MP value of 17.2 kg/m^2.

The tested arrangement of 4 mm thick perforated plates with a 4 mm thick solid plate, class 500 HBW, shows insufficient protective capability against 7.62 × 39 mm API BZ bullets. Both in the case of plates with higher ductility in the areas adjacent to the holes and in the case of plates with lower ductility and higher hardness at the surfaces of the holes compared to the core of the plates, there were single punctures of the perforated plate – solid plate system. Examples of the interaction of a projectile with a perforated plate, characterised by significant plastic deformation at the point of impact, are given in Fig. 15. The only system that passed the multiple firing test includes a perforated plate with reduced ductility and increased hardness of the areas near the edges of the holes relative to the properties of the core of the plate – 4-5f, item 15 in Tab. 4. The way the bullet interacts with the 4-5f plate is by brittle tearing out a large section of the perforated plate, which protects the base plate but leaves a hole of considerable size in the perforated plate – Fig. 16.

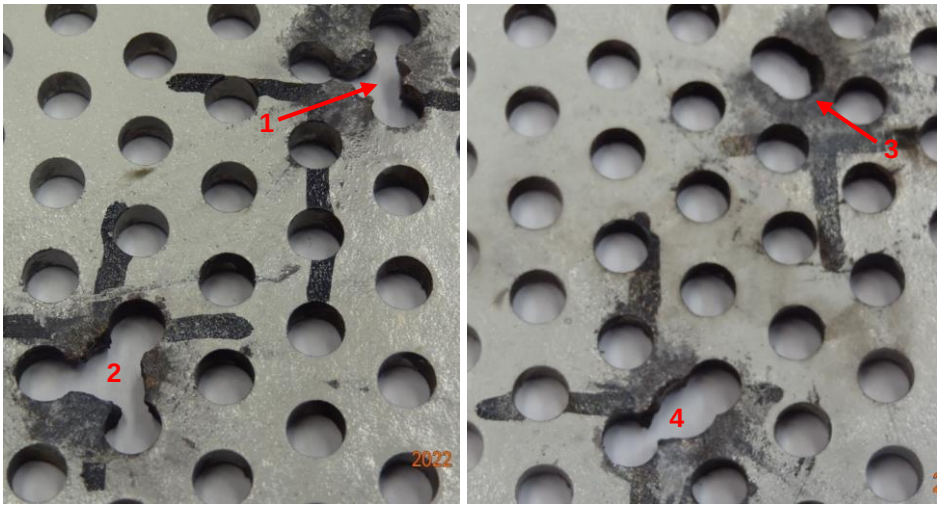

(a) **(b)**

Fig. 15. Plate 4-7f /Per 1-F after OC2: (a) – Shots 1 and 2 / front surface, (b) – Shots 3 and 4 / front surface

Table 4. Summary of the results of multiple-shot tests (multi-hit, STANAG 4569) of perforated plates of nanobainitic steel with a nominal thickness of 4 mm in a baseplate arrangement; the ordinal number and designations of the tested plates, heat treatments and hole making methods – as in Table 2; test result: number of shots not penetrating the solid base plate (+) and number of shots penetrating (-) the solid base plate

Shooting test type	**#**	**Plate design.**	**Pattern D∧T [mm]**	**Test result**	**Traces of the impact of successive bullets on the perforated plate, depending on the point of impact marked in Fig. 3: o- hole, m-bridge, t-triangle, k-edge, n-no identification possible, op-plastic deformation**
Firing of the system: 4 mm perforated plate and 4 mm armour solid plate 500 HBW with 7.62 x 39 mm ammunition API BZ in protection level 2 according to STANAG 4569	11	4-3f/F after OC1	Per 1: 6.0∧10.5	— 3(+), 1(-)	m- punching of bridge, large op edge of tear, fracture (-)t- punching of bridges in the 3-hole area, op of edges m- punching of bridge, large op edge of tear, fracture t- plastic knockout of bridges in the area of the 4-holes
	12	4-4f/F after OC1	Per 2: 6.0∧8.5	— 3(+), 1(-)	(-)k/t- knockout of bridges in the 4-hole area, op t- knockout of bridges in the 4-hole area, op k/t- punching of bridges in the 4-hole area, op t- knockout of bridges in the 4-hole area, op
	13	4-3z-f/L1 before OC2	Per 1: 6.0∧10.5	— 3(+), 1(-)	m- punching of bridge, large op edge of tear, fracture t- plastic punching of bridges in the 3-hole area (-)t-plastic punching of bridge, tear of second bridge m- punching of bridge, large op edge of tear, fracture
	14	4-4z-f/F before OC2	Per 2: 6.0∧8.5	— 3(+), 1(-)	(-)t- plastic punching of bridges in the 4-hole area t- plastic punching of bridges in the 4-hole area n- plastic punching of fragment covering 5 holes t- plastic punching of bridges in the 4-hole area
	15	4-5f/L2 after OC2	Per 1: 6.0∧10.5	+ 4(+)	n- brittle knockout of a fragment involving 5 holes n- brittle knockout of a fragment involving 8 holes n- brittle knockout of a fragment involving 5 holes n- brittle knockout of a fragment involving 5 holes
	16	4-6f/L2 after OC2	Per 2: 6.0∧8.5	— 1(+), 3(-)	(-)n- brittle knockout of a fragment involving 6 holes (-)n- brittle knockout of a fragment involving 6 holes (-)n- brittle knockout of a fragment involving 5 holes (-)n- brittle knockout of a fragment involving 6 holes
	17	4-7f/F after OC2	Per 1: 6.0∧10.5	— 3(+), 1(-)	k/t- plastic punching of bridges in the 3-hole area (-)t- plastic punching of bridges in the 3-hole area k/o- op edges, no cracks m- punching of bridge, large op edge of the tear

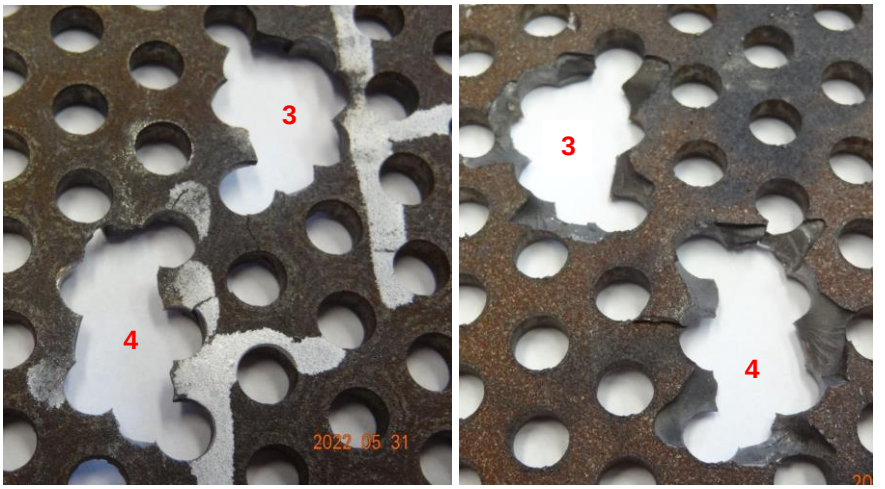

(a) **(b)**

Fig. 16. Plate 4-5f /Per 1-L2 after OC2: (a) – Shots 3 and 4 / front surface, (b) – Shots 3 and 4 / front surface

4.4.3. Firing tests of structure consisting of 8 mm thick perforated plate and the 6 mm thick armour solid plate 500 HBW with 7.62 × 54R mm B32 API ammunition within the scope of protection level 3 according to STANAG 4569

Table 5 gives the results of multi-hit firing tests on eight perforated plates of NB-P nanobainitic steel with a nominal thickness of 8 mm (for actual thicknesses, see Table 2), in terms of protection level 3 according to STANAG 4569 for firing 7.62 × 54R mm B32 API ammunition. Perforations were made by milling (F) or laser beam cutting (L1, L2), using two distances between the centres of the nearest holes: 10.5 mm (T_1) or 8.5 mm (T_2). The areal density of an 8 mm thick solid NB-P steel plate is 62.8 kg/m^2, a perforated plate with parameters [g = 8 mm / D = 6 mm / T = 10.5 mm, ρ = 7.85 g/cm^3] has a surface density of 44.2 kg/m^2, and a plate with parameters [g = 8 mm / D = 6 mm / T = 8.5 mm, ρ = 7.85 g/cm^3] has a surface density of 34.4 kg/m^2.

Of the eight system variants tested: an 8 mm thick perforated plate and a 6mm thick class 500 HBW solid plate, the conditions of the multi-hit firing test with 7.62 × 54R mm B32 API ammunition were met by three variants, with one or two punctures occurring in the remaining five four-shot tests. In the case of plate 8-2f (item 18 in Tab. 5) an additional two shots were taken because the measured velocity of the two projectiles in the primary shot sequence was below the lower limit of the required range.

In the series of plates with higher ductility and lower hardness at the corners adjacent to the holes relative to the properties of the plate core, as well as in the case of plates with lower ductility and higher corner hardness at the surfaces of the holes, there were punctures of the system: perforated plate– solid plate. Plates characterised by plastic deformation at the point of projectile impact and small areas of damage were made in accordance with variants 8-2f (Fig. 17a) and 8-4f (Fig. 17b), but for variants with too low hardness of the edges and the layer adjacent to the surface of the holes – as for variants in which heat treatment was applied after the holes were made (variants 8-2z-f/pos. 21 and 8-4z-f/pos. 22 in Tab. 5), there was a puncture of the base plates. In the case of perforated plates, where the mode of impact of the projectile is to brittlely knock out a section of the perforated plate (variants 8-3f, 8-5f, 8-6f in Tab. 5), a positive firing test result was obtained for the 8-5f plate arrangement. Knocking out a large section of the perforated plate protects the base plate from puncture, but holes of considerable size have been created in the perforated plate – Fig. 18.

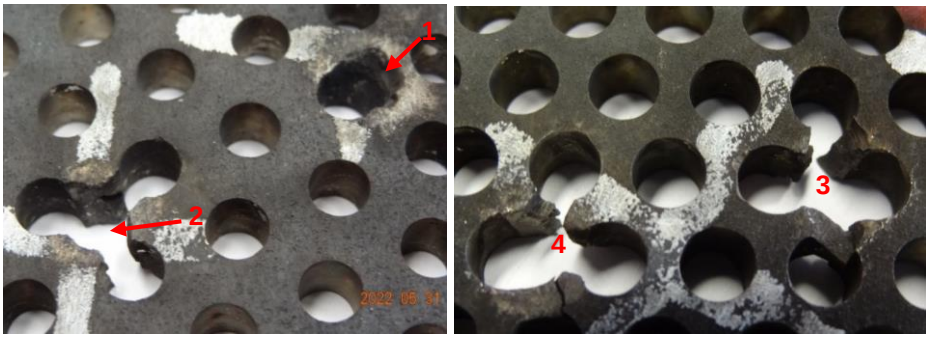

(a) **(b)**

Fig. 17. (a) – Plate 8-2f /Per 1-F after OC1: shots 1 and 2 / front surface, (b) – Plate 8-4f /Per 2-F: shots 3 and 4 / front surface

(a) **(b)**

Fig. 18. Plate 8-5f /Per 1-L2 after OC2: (a) – shot 2 front surface, (b) – shot 2 rear surface

Table 5. Summary of the results of the multi-hit firing tests (STANAG 4569); the ordinal number and designations of the tested plates, heat treatments and hole making methods – as in Tab. 2; test result: number of shots not penetrating the solid base plate (+) and number of shots penetrating the solid base plate (-)

Shooting test type	**#**	**Plate designation**	**Pattern D∧T [mm]**	**Test result**	**Traces of the impact of successive bullets on the perforated plate, depending on the point of impact marked in Fig. 3: o- hole, m-bridge, t-triangle, k-edge, n-no identification possible, op-plastic deformation**
Firing of the system: 8 mm perforated plate and 6 mm armour 500 HBW solid plate with 7.62 x 54R mm B32 API ammunition in protection level 3 according to STANAG 4569	18	8-2f/F after OC1	Per 1: 6.0∧10.5	+ 6(+)	k- edge op, small cavity, no cracks t- knockout of bridges in the 3-hole area, op knockout edges t- knockout of bridges in the 3-hole area, op knockout edges t- knockout of bridges in the 3-hole area, op knockout edges m- partial punching of bridge, op and deflection of tear edges t- knockout of bridges in the 3-hole area, op knockout edges
	19	8-3f/L1 after OC1	Per 1: 6.0∧10.5	— 2(+), 2(-)	t- brittle breakage of the bridges in the 3-hole area (-)o/k- plastic deformation and tear of the hole edges (-)t- brittle breakage of the bridges in the 3-hole area t- brittle breakage of the bridges in the 3-hole area
	20	8-4f/F after OC1	Per 2: 6.0∧8.5	+ 4(+)	t- punching of bridges in the 3-hole area, small op t- punching of bridges in the 4-hole area, small op t- punching of bridges in the 4-hole area, small op t- punching of bridges in the 3-hole area, small op
	21	8-2z-f/F before OC2	Per 1: 6.0∧10.5	— 3(+), 1(-)	(-)t- punching of bridges in the 3-hole area, small op m- punching of bridge, op and deflection of breakout edges m/t- knockout of one bridge and partial knockout of the second, op and bending o- expansion and plastic deformation of the hole
	22	8-4z-f/F before OC2	Per 2: 6.0∧8.5	— 2(+), 2(-)	m/t- knockout of one bridge and partial knockout of the second, op and bending (-)t- punching of bridges in the 3-hole area, small op t- punching of bridges in the 3-hole area, small op (-)t- punching of bridges in the 4-hole area, small op
	23	8-5f/L2 after OC2	Per 1: 6.0∧10.5	+ 4(+)	n- brittle punching involving 3 holes, fracture n- brittle punching involving 3 holes, cracks n- brittle punching involving 3 holes, cracks n- brittle punching involving 4 holes, cracks
	24	8-6f/L2 after OC2	Per 2: 6.0∧8.5	— 3(+), 1(-)	n- brittle punching involving 5 holes, fracture n- brittle punching involving 3 holes, fracture n- brittle knockout covering 7 holes (-)n- brittle-knockout covering 7 holes
	25	8-7f/ F after OC2	Per 1: 6.0∧10.5	— 2(+), 2(-)	(-)t- punching of bridges in the 3-hole area, small op t- punching of bridges in the 3-hole area, op, bending k- significant edge op, no cracks (-)t- punching of bridges in the 3-hole area, op

5. ANALYSIS OF THE RELATIONSHIP BETWEEN THE RESULTS OF FIRING TESTS AND THE PARAMETERS OF THE PERFORATED PLATES

In order to establish a method to increase the protective effectiveness of additional (add-on) armour made of perforated nanobainitic steel plates, the effect of changing selected plate parameters on the way the plates interact with projectiles under multi-hit firing conditions was investigated in three series of tests:

– multi-hit firing of 7.62 ×39 mm API BZ ammunition of 6 mm thick perforated plate with a parallel 500 HBW class 6 mm thick armour-solid plate 40 mm away systems,
– multi-hit firing of 7.62 × 39 mm API BZ ammunition of 4 mm thick perforated plate with a parallel 4 mm thick class 500 HBW solid plate 40 mm away systems,
– multi-hit firing of 7.62 x 54R mm B32 API ammunition of 8 mm thick perforated plate with a parallel 6 mm thick class 500 HBW solid plate 40 mm apart systems.

The influence of the following parameters characterising the manufacturing methods and properties of the perforated plates was studied:

– two hole-making methods: milling (F) and laser beam cutting (L1 – with oxygen as process gas, L2 – with nitrogen as process gas),
– two levels of mechanical properties close to the optimum values achievable for NB-P nanobainitic steel, produced by heat treatment in variants OC1 and OC2 (in Tab. 1),
– sequence of heat treatment and making perforation in plates,
– two types of perforation pattern based on an equilateral triangle, with the same hole diameter of 6.0 mm, differing in pitch values: T_1 = 10.5 mm and T_2 = 8.5 mm.

On the basis of an analysis of the effects of the interaction of the projectiles with the tested perforated plates in the form of plastic deformations, cracks, breaches and tears and marks on the parallel base plates, the influence of the mentioned manufacturing methods and geometrical parameters of the perforated plates on the change in their protective effectiveness was determined.

Methods of making holes

Making holes by machining, under conditions that prevent the material from heating above about 200°C, does not change the microstructure and properties of the heat-treated plates. This ensures that the mechanical properties in the edge area and in the layer adjacent to the surface of the holes remain unchanged from those after the final heat treatment.

By cutting holes with a laser beam, a layer of material is melted and – as a consequence – a remelted and subsequently solidified layer is produced in the volume of material adjacent to the cut surface, as well as a phase-transformed layer with significantly different properties to those of the plate.

In nanobainitic steel plates, the remelted layer and the layer after phase transformation have a higher hardness of 100-150 HV / HBW and lower ductility compared to the material properties of the plate core. This results in the nucleation of cracks during the impact of the projectile, the propagation of which is responsible for the formation of brittle knockouts of large sections of the perforated plate, which is unacceptable under conditions of multi-hit firing.

Mechanical properties of plates controlled by heat treatment parameters

Differences in the mechanical properties of the plates as a result of the OC1 or OC2 treatment variants did not significantly affect the effects of the projectile on the plate. The OC2 variant provides more favourable mechanical properties under firing conditions because, with comparable hardness, the material has higher ductility. The sequence of heat treatment and perforation affects the mechanical properties of the material layers adjacent to the edges and surfaces of the holes. When heat treatment is carried out prior to making holes, the final properties of the material adhering to the surface of the holes are formed during the hole-making process, whereas heat treatment after hole-making leads to a significant reduction in the hardness of the edges and layers near the surface of the holes, with values in the range of 100–150 HV / HBW. The results of the firing tests carried out indicate that the reduced hardness and increased ductility in the material adjacent to the surface of the hole adversely affects the protective properties of the perforated plate, due, among other things, to the more frequent breaking of the bridges during bullet impact.

Perforation pattern, hole diameter and thickness of perforated plates

The influence of the pitch T for the adopted perforation pattern on the protective effectiveness should be considered simultaneously with the influence of the hole size in the perforated plate and the thickness of the plate, under the applied firing conditions with the specific type of ammunition.

In a series of tests with multi-hit firing of 7.62 × 39 mm API BZ ammunition (protection level 2 according to STANAG 4569) of 6 mm thick perforated plate with a parallel 500 HBW class armour solid plate of 6 mm thickness 40 mm away systems, all tested systems met the test criteria. In the final system, the identified cases of the core or large fragments of the projectile core entering through the hole in the perforated plate (example shot 3, Figure 13 a) should be eliminated by reducing the diameter of the hole. Based on the analysis of the results obtained, the proposed final perforation pattern of the 6 mm thick nanobainitic steel plate, which together with the 6 mm thick armour steel base plate of class 500 HBW should provide level 2 ballistic protection, is as follows: D = 5.8 mm, T = 8.5 mm – based on an equilateral triangle.

For a perforation with the aforementioned parameters, the amount of open area is $P = 42.2\%$ and the areal density of the perforated plate is MP = 27.2 kg/m^2. None of the variants of the 4 mm thick perforated plate arrangement with the 4 mm thick solid plate of the 500 HBW class passed the multi-hit firing test with 7.62 × 39 mm API BZ bullets (apart from test no. 15 – Tab. 4, with large knockout areas). In the tests, there were isolated penetrations of the perforated plate– solid plate system. The proposed revised perforation pattern for tests verifying the fulfilment of Level 2 protection is as follows: $D = 5.8$ mm, $T = 10.5$ mm – based on an equilateral triangle, resulting in an open area figure of $P = 27.7\%$ and areal density of the perforated plate of MP = 22.7 kg/m^2.

The multi-hit criterion for Level 3 ballistic protection with 7.62 × 54R mm B32 ammunition API perforated plate with a nominal thickness of 8 mm with a parallel class 500 HBW solid plate with a thickness of 6 mm spaced 40 mm apart systems, was met by perforated plate variants made according to optimised technology with an actual thickness equal to or greater than 8.0 mm (items 18 and 20 in Tab. 5). From the analysis of the results of the firing tests, the following perforation pattern was selected to test the ability to meet the full range of Level 3 ballistic protection requirements of the system [8 mm thick perforated plate made of NB-P steel / solid armour plate class 500 HBW]: $D = 5.0$ mm, $T = 8.5$ mm – based on an equilateral triangle, with an open area value of $P = 31.4\%$ and a perforated panel areal density of MP = 43.1 kg/m^2.

6. SUMMARY AND CONCLUSIONS

As a result of the materials investigation and firing tests, methods were established to increase the protective effectiveness of the additional (add-on) armour of perforated plates made of ultra-high-strength nanobainitic steel with increased ductility compared to the currently used plates with a martensitic structure. The influence of plate production parameters on the manner of interaction with projectiles was investigated, under conditions of multi-hit firing in accordance with STANAG 4569 and AEP-55 vol. 1, with limitations related to dimensions of the tested plates. The influence of the following parameters was studied:

- hole-making method: milling and laser beam cutting,
- mechanical properties of the plates close to the optimum values achievable for NB-P nanobainitic steel, produced by applying two heat treatment variants,
- sequence of heat treatment and perforation of plates,
- triangular perforation pattern, with the same hole diameter of 6.0 mm and centre distances of the nearest holes: 10.5 mm and 8.5 mm.

The influence of the mentioned manufacturing methods and geometrical parameters of the plates on their protective effectiveness based on analysis of the effects of the interaction of the projectiles with the perforated plates tested was established.

Making holes by milling does not change the microstructure and properties of the heat-treated plates. This ensures that the mechanical properties in the edge area and in the layer adjacent to the surface of the holes are unchanged from those after the final heat treatment. By cutting holes with a laser beam, a layer of material is melted and – as a consequence – a remelted and subsequently solidified layer is produced in the volume of material adjacent to the cut surface, as well as a phase-transformed layer with significantly different properties to those of the plate material. This results in the nucleation of cracks during the impact of the projectile, the propagation of which is responsible for the formation of brittle knockouts of large sections of the perforated plate.

The sequence of heat treatment and perforation affects the mechanical properties of the material layers adjacent to the edges and surfaces of the holes. When heat treatment is carried out before the holes are formed, the final properties of the material adhering to the surface of the holes are shaped during the hole-creation process, while post-hole heat treatment leads to a significant reduction in the hardness of the edges and layers near the surface of the holes. Reduced hardness in the material adjacent to the surface of the hole adversely affects the protective properties of the perforated plate.

In a series of multi-hit firing tests with 7.62 × 39 mm API BZ ammunition (protection Level 2 according to STANAG 4569) of 6 mm thick perforated plate with a parallel 500 HBW class armour solid plate of 6 mm thickness 40 mm away systems, all tested systems met the test criteria. In the final system, the identified cases of the core or large fragments of the projectile core entering through the hole in the perforated plate should be eliminated by reducing the diameter of the hole.

In multi-hit firing tests of a 4 mm thick perforated plate with a 4 mm thick solid plate of 500 HBW class system with 7.62 × 39 mm API BZ ammunition (protection Level 2 according to STANAG 4569), there were single penetrations of the perforated plate – solid plate system. A revised perforation pattern has been proposed for testing to verify the fulfilment of Level 2 protection: D = 5.8 mm, T = 10.5 mm – based on an equilateral triangle.

The multi-hit criterion for Level 3 ballistic protection with 7.62 × 54R mm B32 API ammunition was met by perforated 8 mm thick plate combined with a parallel solid 6 mm thick plate of class 500 HBW 40 mm away. In order to verify that the full range of Level 3 ballistic protection requirements are met for a system with an 8 mm thick perforated plate, the following perforation pattern was specified: D = 5.0 mm, T = 8.5 mm - based on an equilateral triangle.

FUNDING

The research, the results of which are presented in this article, was carried out as part of Project No. 1/Ł- IMŻ/CŁ/2021 "Development of technology and production of perforated armour plates from ultra-high-strength nanobainitic steel" funded by a grant from the Łukasiewicz Centre (Poland).

REFERENCES

[1] European Patent Application no 86303640.6. 1986. *An armour assembly for armoured vehicles*. Date of filing: 13.05.1986.
[2] United States Patent no 5,014,593. 1989. *Perforated plate armor*. Filed: Oct. 18, 1989.
[3] Børvik, Tore, M.J. Forrestal, and T.L. Warren. 2009. "Perforation of 5083-H116 aluminum armor plates with ogive-nose rods and 7.62 mm APM2 bullets". *Experimental Mechanics* 50 (7) : 969-978.
[4] Balos, Sebastian, Vencislav Grabulov, Leposava Sidjanin, Mladen Pantic, and Igor Radisavljevic. 2010. "Geometry, mechanical properties and mounting of perforated plates for ballistic application". *Materials and Design* 31 (6) : 2916-2924.
[5] MIL-PRF-32269 (MR). 2007. *Performance Specification-Perforated Homogeneous Steel Armor*. 18 October 2007.
[6] Chocron, Sidney, Charles E. Anderson Jr., Donald J. Grosch, and Carl H. Popelar. 2001. "Impact of the 7.62-mm APM2 projectile against the edge of a metallic target". *International Journal of Impact Engineering* 25 : 423-437.
[7] United States Patent Application no 11A290,451. 2005. *Perforated Armor Plates*. Filed: Dec. 1, 2005.
[8] International Patent Application no PCT/US2009/045700. 2009. *Perforated Armor with Geometry Modified for Lighter Weight*. Filed: May 29, 2009.
[9] Wiśniewski, Adam, and Paweł Żochowski. 2013. "Add-on passive armour for light armoured vehicles protection". *Problemy Techniki Uzbrojenia* 42 (125) : 17-24.
[10] Stępniak, Wiesław, Wiesław Habaj, and Paweł Podgórzak. 2014. „Pancerze perforowane". *Problemy Mechatroniki. Uzbrojenie, lotnictwo, inżynieria bezpieczeństwa* 5 (1) : 59-70.
[11] https://industeel.arcelormittal.com/news/fichier/ds-protection-mars-650-perforated-en-2021/.
[12] www.miilux.fi/esitteet/protection500_perforated_datasheet_miilux.pdf.
[13] https://ploughshare.co.uk/wp-content/uploads/2021/09/Super-Bainite-Steel.pdf.

[14] ISO 286-2:2010(E) *Geometrical product specifications (GPS) – ISO code system for tolerances on linear sizes — Part 2: Tables of standard tolerance classes and limit deviations for holes and shafts*.
[15] ISO 9013 Second edition 2002-09-15 *Thermal cutting – Classification of thermal cuts – Geometrical product specification and quality tolerances*.
[16] Balos, Sebastian, Daniel Howard, Adrian Brezulianu, and Danka Labus Zlatanović. 2021. "Perforated Plate for Ballistic Protection—A Review". *Metals* 11 (4) : 526-1-18.
[17] Hazell, J. Paul, Gareth J. Appleby-Thomas, D. Philbey, and W. Tolman. 2013. "The effect of gilding jacket material on the penetration mechanics of a 7.62 mm armour-piercing projectile". *International Journal of Impact Engineering* 54 : 11-18.
[18] Lesmana, Denny, Faizal Arifurrahman, Amer Hameed, Gareth J. Appleby-Thomas, and Sigit P. Santosa. 2020. "On the importance of the bullet jacket during the penetration process: Reversed-ballistic experimental and numerical study". *Journal of Mechanical Science and Technology* 34 (5) : 1871-1877.
[19] Balos, Sebastian, Igor Radisavljevic, Petar Janjatovic, Miroslav Dramicanin, Olivera Eric-Cekic, and Leposava Sidjanin. 2019. "Ballistic Behaviour of Austempered Compacted Graphite Iron Perforated Plates". *Defence Science Journal* 69 (6) : 571-576.
[20] Radisavljevic, Igor, Sebastian Balos, Milutin Nikacevic, and Leposava Sidjanin. 2013. "Optimization of geometrical characteristics of perforated plates". *Materials and Design* 49 : 81-89.
[21] Kilic, Namik, Said Bedir, Atil Erdik, Bulent Ekici, Alper Tasdemirci, and Mustafa Güden. 2014. "Ballistic behavior of high hardness perforated armor plates against 7.62 mm armor piercing projectile". *Materials and Design* 63 : 427-438.
[22] Kilic, Namik, Bulent Ekici, and Said Bedir. 2016. "Optimization of high hardness perforated steel armor plates using finite element and response surface methods". *Mechanics of Advanced Materials and Structures* 24 (7) : 615-624.
[23] Mishra, Bidyapati, B. Ramakrishna, Pradipta Kumar Jena, K. Siva Kumar, Madhu Vemuri, and N.K. Gupta. 2013. "Experimental studies on the effect of size and shape of holes on damage and microstructure of high hardness armour steel plates under ballistic impact". *Materials and Design* 43 : 17-24.
[24] Mishra, Vaibhav, and Vikas Kukshal. 2022. Ballistic Performance of Circular and Oval Shape Perforated Metallic Armour. In: *Composite Materials for Extreme Loading*- Proceedings of the Indo-Korean workshop on Multi Functional Materials for Extreme Loading 2021(eds: Shankar Krishnapillai, Velmurugan R., and Sung Kyu Ha). Springer, Singapore.

[25] Fras, Teresa, A. Murzyn, and Piotr Krzysztof Pawlowski. 2017. "Defeat mechanisms provided by slotted add-on bainitic plates against small-calibre 7.62mm AP projectiles". *International Journal of Impact Engineering* 103: 241-253.

[26] Fras, Teresa, Christian C. Roth, and Dirk Mohr. 2018. "Fracture of high-strength armor steel under impact loading". *International Journal of Impact Engineering* 111: 147-164.

[27] Saragosa, James. 2015. *Design and Characterization of a Nanoscale Carbide-Free Bainite Alloy*. A Thesis for the Degree Master of Science. McMaster University, Hamilton, Ontario.

[28] Garbarz, Bogdan, and Wojciech Burian. 2014. "Microstructure and Properties of Nanoduplex Bainite-Austenite Steel for Ultra-High-Strength Plates". *Steel Research International* 85 (12) : 1620-1628.

[29] Garbarz, Bogdan, Jarosław Marcisz, Krzysztof Żółkiewski, Paweł Lubowiecki, Bogusław Nowak, Marek Smoleń, and Marcin Skurczyński. 2020. "Industrial technology of manufacturing of ultra-strength nanobainitic steel plates". *Journal of Metallic Materials* 72 (2) : 2-22.

[30] Marcisz, Jarosław, Bogdan Garbarz, Jerzy Stępień, Tymoteusz Tomczak. Lech Starczewski, Robert Nyc, Michał Gmitrzuk, and Marcin Gołuński. 2020. "Protective effectiveness of armour made of nanobainitic steel". *Journal of Metallic Materials* 72 (1) : 21-38.

[31] Marcisz, Jarosław, Bogdan Garbarz, Aleksandra Janik, and Władysław Zalecki. 2021. "Controlling the Content and Morphology of Phase Constituents in Nanobainitic Steel Containing 0.6%C to Obtain the Required Ratio of Strength to Plasticity". *Metals* 11 (4) : 658-1-21.

[32] Burian, Wojciech, Jarosław Marcisz, Lech Starczewski, and Małgorzata Wnuk. 2017. "A Probabilistic Model of Optimising Perforated High-Strength Steel Sheet Assemblies for Impact-Resistant Armour Systems". *Problemy mechatroniki. Uzbrojenie, lotnictwo, inżynieria bezpieczeństwa /Problems of Mechatronics. Armament, Aviation, Safety Engineering* 8 (1) : 71-88.

[33] Burian, Wojciech, Paweł Żochowski, Michał Gmitrzuk, Jarosław Marcisz, Lech Starczewski, Barbara Juszczyk, and Mariusz Magier. 2019. "Protection effectiveness of perforated plates made of high strength steel". *International Journal of Impact Engineering* 126 : 27-39.

[34] https://imz.pl/pl/aktualnosci.php?wid=33&news=253 *Walcarka do walcowania na gorąco wraz z urządzeniami do obróbki cieplnoplastycznej (moduł B-LPS).*

Metody zwiększenia skuteczności ochronnej dodatkowego pancerza z perforowanych blach z ultra-wytrzymałej stali nanobainitycznej

Bogdan GARBARZ[1], Jarosław MARCISZ[1], Wojciech BURIAN[2], Aleksander KOWALSKI[2], Jacek BOROWSKI[3], Szymon SZKUDELSKI[3], Marek WALICKI[4], Kamil ZAJĄC[4]

[1]Sieć Badawcza Łukasiewicz – Górnośląski Instytut Technologiczny ul. Karola Miarki 12-14, 44-100 Gliwice,
[2] Sieć Badawcza Łukasiewicz – Instytut Metali Nieżelaznych ul. Sowińskiego 5, 44-100 Gliwice,
[3] Sieć Badawcza Łukasiewicz – Poznański Instytut Technologiczny ul. Ewarysta Erdkowskiego 6., 61-755 Poznań,
[4]CFT Precyzja sp. z o.o., ul. Polna 6, 05-152 Czosnów

Streszczenie. Celem badań było opracowanie technologii wytwarzania płyt perforowanych ze stali nanobainitycznej o skuteczności ochronnej konkurencyjnej w stosunku do obecnie dostępnych pancernych płyt perforowanych. Płyty perforowane o wymiarach 300 × 260 mm × (4 mm, 6 mm oraz 8 mm) wytworzono ze średniostopowej stali nanobainitycznej zawierającej 0,6% masowych węgla. Wykonano badania metalograficzne za pomocą mikroskopu świetlnego i skaningowego mikroskopu elektronowego oraz pomiary mikrotwardości i twardości. Testy ostrzałem wykonano wg STANAG 4569:ed3:2014 zgodnie z procedurą dostosowaną do wymiarów badanych płyt perforowanych. Wykonanie otworów w płytach metodą obróbki skrawaniem nie zmieniło właściwości mechanicznych w warstwach materiału przylegających do otworów. Wycinanie otworów laserem spowodowało spadek ciągliwości i w rezultacie zarodkowanie pęknięć w trakcie uderzenia pocisku. Wszystkie warianty układów płyt perforowanych o grubości 6 mm z płytami litymi o grubości 6 mm 500 HBW badane ostrzałem amunicją 7,62 × 39 mm-API-BZ spełniły wymagania poziomu 2 STANAG 4569. Układy płyt perforowanych o grubości 4 mm z płytą litą o grubości 4 mm 500 HBW nie spełniły wymagań poziomu 2. W wyniku ostrzału amunicją 7,62 × 54R mm-B32-API układów płyt perforowanych o grubości 8 mm z równoległymi płytami litymi 500 HBW o grubości 6 mm w zakresie poziomu 3 STANAG 4569, uzyskano pozytywne rezultaty dla określonych wariantów. Zaproponowano zmodyfikowane wzory perforacji dla płyt nanobainitycznych do finalnej weryfikacji eksperymentalnej.

Słowa kluczowe: dodatkowe opancerzenie, stalowe płyty perforowane, ultra-wytrzymała stal nanobainityczna